

# 1. INTRODUCTION AND EXPLANATORY NOTES<sup>1</sup>

## Shipboard Scientific Party<sup>2,3</sup>

### INTRODUCTION

Understanding the complex and interrelated volcanic, tectonic, and hydrothermal processes occurring at oceanic spreading centers, where two thirds of the Earth's crust is created, is one of the highest priority scientific questions addressed by the Ocean Drilling Program (ODP). Although much has been learned about these spreading-center processes from detailed geological and geophysical investigations over the past decade

(e.g., the FAMOUS, AMAR, RISE, Galapagos, and Juan de Fuca studies), there are many fundamental questions regarding magma genesis, oceanic petrology, hydrothermal circulation, and crustal magnetization that can only be answered by direct sampling in deep crustal drill holes. Recent studies have shown that the accretionary zone where these geological processes are concentrated is remarkably narrow, averaging only a few kilometers in width (Macdonald, 1982). Thus, in order to study the formation of new oceanic lithosphere at mid-ocean ridges, drilling is required within the narrow, zero-age crust of the accretionary zone itself.

Since Leg 37 of the Deep Sea Drilling Project (DSDP) first demonstrated the feasibility of drilling to substantial depths within the oceanic crust, numerous basement holes have been attempted on very young (< 1-m.y.-old) seafloor, without notable success. For example, the average penetration of the 12 basement holes attempted on DSDP Leg 54 on the East Pacific Rise and Galapagos Spreading Center was 21 m, and many of the holes had to be abandoned at much shallower depths, with core recovery averaging only about 19% (Natland and Rosendahl, 1980). The seven young-basement holes drilled on the south flank of the Galapagos Spreading Center on Leg 70 were no more successful, with a maximum penetration of only 10 m and core recovery less than 7% (Honnorez, Von Herzen, et al., 1983). The majority of these holes had to be abandoned after only a few meters of penetration owing to premature bit destruction, frictional binding, and extreme torquing of the drill string and continual sloughing of rock debris into the hole. Moreover, the requirement for significant thicknesses of sediment (> 100 m) on the basement in order to spud-in precluded any drilling within the very young, largely sediment-free accretionary zone.

In light of these problems and the importance of drilling at mid-ocean ridges, the COSOD report (COSOD, 1981) and the JOIDES Planning Committee recommended the development of new technology for drilling young, fresh volcanic rocks in areas with little or no sediment cover. Texas A&M University, as the science operator for the Ocean Drilling Program, had been developing these bare-rock drilling techniques. A specially designed guidebase was constructed to provide lateral support for the drill string during bare-rock spud-in, and new drilling and coring techniques were developed for use in the hard, highly abrasive, fractured volcanic rocks found at mid-ocean ridges. It was considered essential to test and evaluate this new drilling technology early in the Ocean Drilling Program and establish one or more crustal drill holes at both fast- and slow-spreading centers. As a first step toward achieving this objective, Legs 106 and 109 were dedicated to establishing the first hole in zero-age crust in a well-studied portion of the Mid-Atlantic Ridge rift valley, south of the Kane Fracture Zone (Fig. 1).

### Scientific Objectives

Important scientific questions addressed by a drill hole in zero-age crust at a slow-spreading ridge include the following:

1. The composition and relative abundance of the parental magmas at a slow-spreading ridge and their relation to the "evolved" basalts erupted at the seafloor.

<sup>1</sup> Shipboard Scientific Party, 1988. *Proc. ODP, Init. Repts. (Pt. A)*, 106/109: College Station, TX (Ocean Drilling Program).

<sup>2</sup> Robert S. Detrick (Co-Chief Scientist), Graduate School of Oceanography, University of Rhode Island, Kingston, RI 02881; Jose Honnorez (Co-Chief Scientist), Rosenstiel School of Marine and Atmospheric Sciences, University of Miami, 4600 Rickenbacker Causeway, Miami, FL 33149 (current address: Institut de Géologie, Université Louis Pasteur, 1 Rue Blessig, 67084 Strasbourg, France; Andrew C. Adamson (Staff Scientist), Ocean Drilling Program, Texas A&M University, College Station, TX 77843; Garrett W. Brass, Ocean Drilling Program, National Science Foundation, 1800 G Street NW, Washington, DC 20550; Kathryn M. Gillis, Department of Geology, Dalhousie University, Halifax, Nova Scotia B3H 3J5, Canada (current address: Département de Géologie, Université de Montréal, C.P. 6128, Succursale A, Montréal, Québec H3C 3J7, Canada); Susan E. Humphris, Department of Chemistry, Woods Hole Oceanographic Institution, Woods Hole, MA 02543; Catherine Mevel, Laboratoire de Pétrologie Métamorphique, Université Pierre et Marie Curie, 4 Place Jussieu, 75230 Paris 05, France; Peter S. Meyer, Department of Geology and Geophysics, Woods Hole Oceanographic Institution, Woods Hole, MA 02543; Nikolai Petersen, Institute für Geophysik, Universität München, Theresienstrasse 41, D-8000 München 2, Federal Republic of Germany; Martina Rautenschlein, Max-Planck-Institut für Chemie, Abteilung Geochemie, Postfach 3060, D-6500 Mainz, Federal Republic of Germany; Tsugio Shibata, Faculty of Science, Okayama University, 3-1-1 Tsushima-naka, Okayama 700, Japan; Hubert Staudigel, Geological Research Division, Scripps Institution of Oceanography, University of California, San Diego, La Jolla, CA 92093; Anita L. Woodlridge, Marine Geology and Geophysics, University of Miami, 4600 Rickenbacker Causeway, Miami, FL 33149; Kiyohiko Yamamoto, Faculty of Science, Tohoku University, Sendai, Miyagi Pref. 980, Japan.

<sup>3</sup> Wilfred B. Bryan (Co-Chief Scientist), Department of Geology and Geophysics, Woods Hole Oceanographic Institution, Woods Hole, MA 02543; Thierry Juteau (Co-Chief Scientist), Laboratoire de Pétrologie, Université de Bretagne Occidentale, 6 Avenue Le Gorgeu, 29287 Brest, France; Andrew C. Adamson (ODP Staff Scientist), Ocean Drilling Program, Texas A&M University, College Station, TX 77843; Laurie K. Autio, Department of Geology and Geography, Morrill Science Center, University of Massachusetts, Amherst, MA 01003; Keir Becker, Rosenstiel School of Marine and Atmospheric Sciences, University of Miami, 4600 Rickenbacker Causeway, Miami, FL 33149; M. Mansour Bina, Laboratoire de Géomagnétisme, Université Pierre et Marie Curie, 4, Avenue de Neptune, 94107 St. Maur des Fosses, France; Jean-Philippe Eissen, O.R.S.T.O.M., B.P. A5, Noumea, New Caledonia (current address: O.R.S.T.O.M., IFREMER, BP 337, 2273 Brest Cedex, France); Toshitsugu Fujii, Earthquake Research Institute, University of Tokyo, 1-1-1 Yayoi, Bunkyo-ku, Tokyo 113, Japan; Timothy L. Grove, Department of Earth, Atmospheric and Planetary Sciences, Massachusetts Institute of Technology, Cambridge, MA 02139; Yozo Hamano, Earthquake Research Institute, University of Tokyo, 1-1-1 Yayoi, Bunkyo-ku, Tokyo 113, Japan; Rejean Hebert, Département de Géologie, Université Laval, Québec G1K 7P4, Canada; Stephen C. Komor, Bureau of Mines, Avondale Research Center, 4900 LaSalle Road, Avondale, MD 20782 (current address: Department of Geology and Geophysics, University of Wisconsin, Madison, WI 53706); Johannes Kopietz, Bundesanstalt für Geowissenschaften und Rohstoffe, Stillweg 2, D-3000 Hannover 51, Federal Republic of Germany; Kristian Kramer, Institut für Geophysik, Universität München, Theresienstrasse 41, D-8000 München 2, Federal Republic of Germany; Michel Loubet, Laboratoire de Mineralogie, Université Paul Sabatier, 38 Rue des 36 Ponts, 31400 Toulouse, France; Daniel Moos, Borehole Research Group, Lamont-Doherty Geological Observatory, Columbia University, Palisades, NY 10964; Hugh G. Richards, Department of Geology, The University, Newcastle upon Tyne NE1 7RU, United Kingdom.

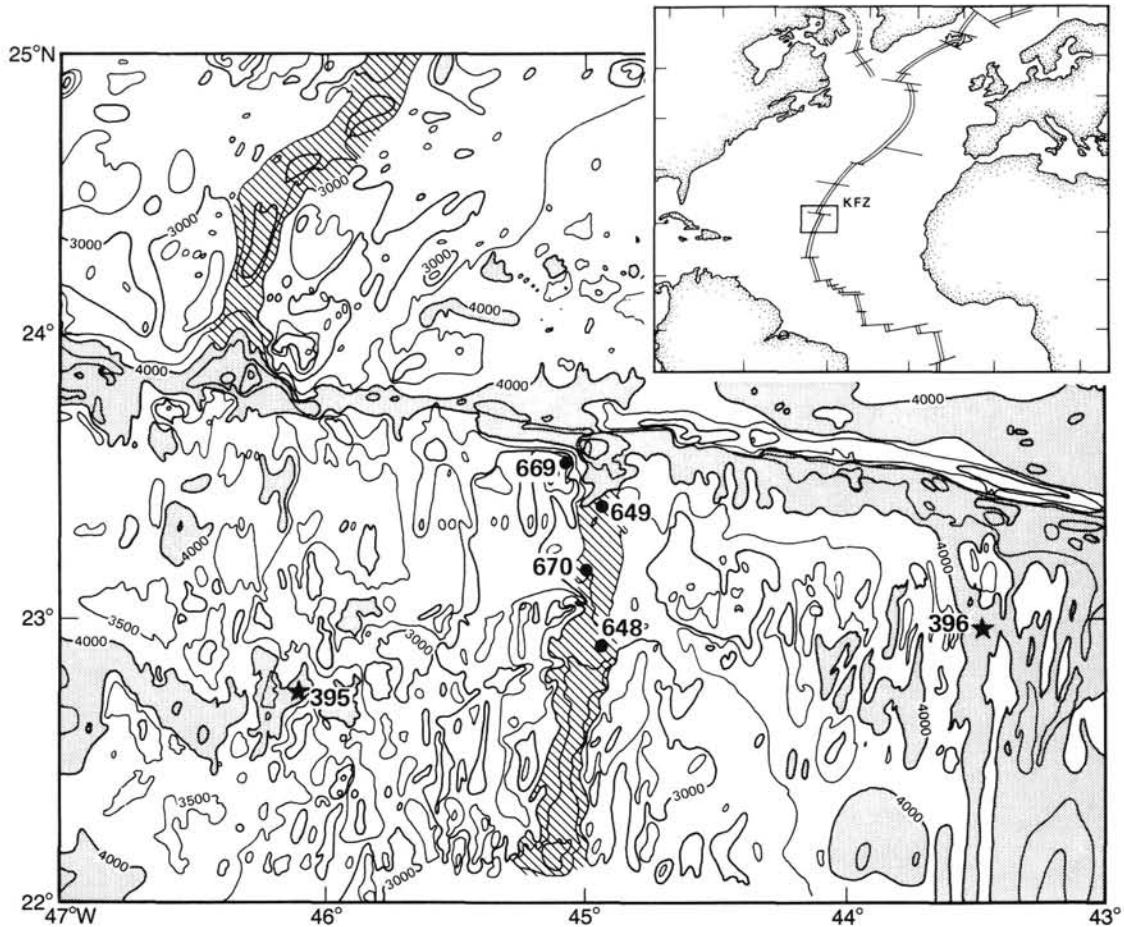


Figure 1. Bathymetric map of the Kane Fracture Zone showing the location of the drill sites occupied on Legs 106 and 109. Contour interval, 500 m. ODP sites marked by dots, DSDP sites by stars. Location of Mid-Atlantic Ridge shown by diagonal lines (redrawn from Detrick and Purdy, 1980).

2. The variation in magma generation and crustal accretion rates in time and space and how these magmatic processes are linked to tectonic and hydrothermal activity within the rift valley.

3. The depth to the top of an axial magma chamber and the nature of the compositional variations within the chamber.

4. The effect of transforms on crustal accretion processes at a slow-spreading ridge.

5. The duration and extent of hydrothermal activity within the rift valley and the imprint of this activity on the alteration history of oceanic crust.

6. The nature of the root zone of an active hydrothermal system: the mineralogy and chemistry of vein filling and the nature and extent of alteration of adjacent basalts.

7. The nature of the earliest low-temperature alteration of zero-age basalts and its effects on crustal mineralogy.

8. The variation of crustal magnetization with depth in newly accreted crust and how it is affected by hydrothermal and tectonic processes in the rift valley.

In addition to these specific questions, a crustal drill hole at a mid-ocean ridge offers a unique opportunity for a variety of downhole geophysical experiments and long-term monitoring of accretionary processes. This is a first step toward establishing a natural laboratory where geological processes at oceanic spread-

ing centers can be studied using many different kinds of down-hole instrumentation over an extended period of time.

### Engineering Objectives

The difficulties previously experienced with crustal drilling on very young seafloor are probably due to a combination of factors, the most important of which are (1) lack of detailed drill site information (local slope, roughness, type of exposed rock, and tectonic setting); (2) inability to spud-in owing to buckling of an unsupported bottom-hole assembly; (3) very slow penetration rates and excessive bit wear owing to the presence of fresh, glassy volcanic rocks that are extremely hard, very abrasive, and highly fractured; and (4) severe hole instability, leading to frictional binding and torquing of the drill string in fractured basaltic rubble.

In recognition of these problems, a number of new or previously untested systems were planned for use on Legs 106 and 109. These included the following:

1. A high-resolution, 360°, color sonar tool imaging the seafloor and aiding in reentry operations.

2. A low light intensity black-and-white video camera system for visual observation of the seafloor and drilling operations.

3. A hard-rock guidebase (HRGB) to confine the bit during the initial spud-in operation.
4. A system for lowering the guidebase to the seafloor, releasing it, and cementing it.
5. Downhole drilling and coring motors to facilitate bare-rock spud-in and to allow coring in the shallow part of the section.
6. A wireline-retrievable core system compatible with the coring motor.
7. Special "hard formation" coring bits.
8. A modified reentry cone with a gimbaled seat for deployment in the HRGB.
9. Specially formulated cements and muds to assist in stabilizing or cleaning drill holes.

From an engineering perspective, the main objective of these legs was to test and evaluate these nine new systems, determine their feasibility for bare-rock crustal drilling, and make recommendations for future drilling efforts of this kind.

### Leg 106

On Leg 106, the hard-rock guidebase was successfully deployed at Site 648 in 3344 m of water on the flat summit plateau of a small axial volcano in the Mid-Atlantic Ridge rift valley, about 70 km south of the Kane Fracture Zone (Fig. 1). The positive-displacement downhole drilling motors were used to spud-in to the basaltic crust. Despite difficulties with severe hole instability, excessive bit wear, and poor recovery, the hole was advanced to a total depth of 33 m below seafloor before drilling was terminated after 25 days.

Near the end of Leg 106 a real-time video system, acquired to help find sites for deploying the hard-rock guidebase, was used to discover a major, active hydrothermal field (Snake Pit Hydrothermal Area) in the rift valley about 25 km south of the Kane Fracture Zone (Site 649). Ten shallow holes were drilled at this site to sample the hydrothermal deposits and the underlying basement rocks.

### Leg 109

The principal objective of Leg 109 was to re-occupy and deepen Hole 648B, at least until a significant lithologic boundary was crossed. Technical improvements, based on the Leg 106 experience, included emphasis on 9 7/8-in. core bits, greater armoring on the outer surfaces of all bits used, and special, lightweight, 10 1/4-in. casing with a hanging adapter to fit in to the reentry cone. The smaller bit diameter and armoring were expected to reduce caving, to extend bit life, and to increase the penetration rate. Four specially designed drilling jars were aboard to use in combatting sticking in the hole. Despite these efforts, two failures of the bottom-hole assembly and continued problems with severe hole instability limited the total additional penetration achieved at Hole 648B on Leg 109 to about 17 m. Despite this disappointing result, the core recovered from Hole 648B provided a unique view of the internal plumbing of a small axial volcano.

Another important objective of Leg 109 was logging and downhole experiments at Hole 395A, located about 100 km west of the Mid-Atlantic Ridge rift valley (Fig. 1). Although attempts had been made to log Hole 395A toward the end of Leg 45 and again on Leg 78B, these attempts were only partly successful, and other downhole measurements made on Leg 78B were of questionable quality. Although the lower 55 m of Hole 395A were lost to caving, the hole remains as one of the deepest penetrations into oceanic basement. An excellent set of logging data was obtained on Leg 109 at Hole 395A, including downhole temperature, resistivity, sonic velocity, magnetic polarity, susceptibility, and chemical variation logs. A packer experiment,

which measured the permeability at different levels in the hole, was also successfully carried out.

Two additional sites were drilled on Leg 109. A brief unsuccessful attempt was made to spud-in to gabbro exposed high on the rift valley walls near the Kane transform (Site 669). Later in the leg a large body of serpentinized peridotite, discovered by scientists diving in this same area, was drilled at Site 670. Over 90 m of serpentinized peridotites were drilled at this site, located just a few kilometers from the neovolcanic zone in the Mid-Atlantic Ridge rift valley.

The details and results of these two legs are presented in the site chapters that follow (this volume). The results of specialized studies will be published as the Final Report (Part B) of the Leg 106/109 *Proceedings* volume.

## EXPLANATORY NOTES

### General Information

The following notes are intended to aid interested investigators in understanding the terminology, labeling, and numbering conventions used by the Ocean Drilling Program during Legs 106 and 109. Precedents set by Leg 106 while drilling at Site 648 were generally followed on Leg 109. However, each leg also faced some unique problems. Leg 106 cored and sampled hydrothermal deposits at Site 649, whereas Leg 109 drilled serpentinized peridotite at Site 670. Also, Leg 109 conducted a major logging and downhole measurements program at Site 395. Neither leg drilled the fossiliferous marine sediments for which there are many well-established procedures and conventions. The following discussion and explanation of procedures thus are primarily relevant to drilling that commences on zero-age crust or within an existing hole, as was done on Leg 111 at Hole 504B.

### Authorship of Site Reports

#### Site 648

Authorship of the site reports is shared among the entire shipboard parties of both Leg 106 and Leg 109, although the four co-chief scientists and the staff scientist edited and rewrote part of the material prepared by other individuals. The site chapters are organized as follows (authors are listed in alphabetical order in parentheses; no seniority is necessarily implied):

Site Summary (Bryan, Detrick, Honnorez, Juteau)  
 Background and Objectives (Detrick)  
 Geologic and Tectonic Setting (Detrick)  
 Operations (Howard, Serocki)  
 Lithostratigraphy (Adamson, Juteau)  
 Petrography (Eissen, Fujii, Grove, Hebert, Humphris, Meyer, Rautenschlein, Shibata, Staudigel)  
 Geochemistry (Autio, Brass, Loubet)  
 Alteration (Gillis, Mevel, Richards)  
 Paleomagnetism (Bina, Hamano, Peterson, Wooldridge)  
 Physical Properties (Moos, Krammer, Yamamoto)  
 Thermal Conductivity (Kopietz)  
 Summary and Conclusions (Bryan, Detrick, Honnorez, Juteau)  
 Barrel Sheets/Thin Section Description (Adamson, Eissen, Fujii, Gillis, Grove, Hebert, Humphris, Mevel, Meyer, Rautenschlein, Richards, Shibata, Staudigel)

#### Site 649

Authorship of the site reports is shared among the entire party of Leg 106, although the two co-chief scientists and the staff scientist edited and rewrote part of the material prepared by other individuals. The site chapters are organized as follows

(authors are listed in alphabetical order in parentheses; no seniority is necessarily implied):

Site Summary (Detrick, Honnorez)  
 Background and Objectives (Detrick)  
 Geologic, Tectonic, and Biologic Setting (text: Detrick; map of hydrothermal vent area: Mevel and Rautenschlein)  
 Operations (Serocki)  
 Lithostratigraphy (Adamson)  
 Petrography (Gillis, Humphris, Meyer, Rautenschlein, Shibata, Staudigel) Mineralogy (Honnorez, Mevel)  
 Summary and Conclusions (Detrick, Honnorez)  
 Barrel Sheets/Thin Section Description (Adamson, Gillis, Humphris, Mevel, Meyer, Rautenschlein, Shibata, Staudigel)

#### Site 395

The site chapters are organized as follows:

Site Summary (Becker, Moos)  
 Background (Becker, Moos)  
 Operations (Moos, Becker)  
 Temperature Measurements (Becker, Kopietz, Hamano)  
 Schlumberger Logs (Moos)  
 Multi-channel Sonic Log (Moos)  
 Magnetometer Log (Kopietz, Hamano)  
 Magnetic Susceptibility Log (Krammer)  
 Hydrogeology (Becker)

#### Site 669

Authorship of the site reports is shared among the entire Leg 109 shipboard party, although the two co-chief scientists and the staff scientist edited and rewrote part of the material prepared by other individuals. The site chapters are organized as follows (authors are listed in alphabetical order in parentheses; no seniority is necessarily implied):

Site Summary (Bryan, Juteau)  
 Background and Objectives (Bryan, Juteau)  
 Operations (Howard)  
 Lithostratigraphy (Adamson)  
 Petrography (Eissen, Fujii, Grove, Hebert, Komor)  
 Alteration (Richards)  
 Physical Properties (Krammer, Moos)  
 Thermal Conductivity (Kopietz)  
 Summary and Conclusions (Bryan, Juteau)  
 Barrel Sheets/Thin Section Description (Adamson, Eissen, Fujii, Grove, Hebert, Komor, Richards)

#### Site 670

Authorship of the site reports is shared among the entire Leg 109 shipboard party, although the two co-chief scientists and the staff scientist edited and rewrote part of the material prepared by other individuals. The site chapters are organized as follows (authors are listed in alphabetical order in parentheses; no seniority is necessarily implied):

Site Summary (Bryan, Juteau)  
 Background and Objectives (Bryan, Juteau)  
 Geologic and Tectonic Setting (Bryan, Juteau)  
 Operations (Howard)  
 Lithostratigraphy (Adamson, Juteau)  
 Petrography (Eissen, Fujii, Grove, Hebert, Juteau, Komor, Richards)  
 Paleomagnetism (Hamano, Bina)  
 Physical Properties (Krammer, Moos)  
 Thermal Conductivity (Kopietz)

Summary and Conclusions (Bryan, Juteau)  
 Barrel Sheets/Thin Section Description (Adamson, Eissen, Fujii, Grove, Hebert, Komor, Richards)

#### Numbering of Sites, Holes, Cores, and Samples

ODP drill sites are numbered consecutively from the first site drilled by *Glomar Challenger* in 1968. A site number refers to one or more holes drilled while the ship is positioned over one acoustic beacon. Multiple holes may be drilled at a single site by pulling the drill pipe above the seafloor (out of one hole), moving the ship some distance from the previous hole, and then drilling another hole.

The first hole drilled at an ODP site is assigned the site number modified by the suffix A. Subsequent holes at the same site are designated with the site number modified by letters of the alphabet assigned in chronological sequence of drilling. Note that this differs slightly from the DSDP practice of designating the first hole at a given site by the site number, unmodified, and subsequent holes by the site number modified by letters of the alphabet (for example, Hole 504B, originally drilled by DSDP, was the third hole that DSDP drilled at Site 504). It is important, for sampling purposes, to distinguish among the holes drilled at a site, because recovered sediments or rocks from different holes usually do not come from equivalent positions in the stratigraphic column.

Three varieties of coring systems were employed during Legs 106 and 109. The rotary-coring system (RCB) was the basic system used for coring basalts. Two types of coring motors were used on the lower end of the drill string. The positive-displacement coring motor (PDCM) permits drilling with rotation of only the bottom-hole assembly; core may be recovered by wireline as with the rotary system. The positive-displacement drilling motor (PDM) has a similar drilling capability but the complete bottom-hole assembly must be brought to the surface to recover core. Rotary-drilled cores are designated by an R in ODP core and sample identifiers; cores recovered with either of the coring motors are designated by a D. On Leg 106, an attempt was made to use an Extended Core Barrel system (XCB) with a drilling motor. This device did not recover significant samples; if successful, such cores would be designated by an X. If loose cuttings washed out of the upper part of the hole are recovered in a core, they are identified by a W.

The RCB, which is the standard coring device used since DSDP Leg 1, was used with roller-cone bits reinforced with additional carbide hard-facing on Leg 109. Ideally, a core approximately 9.5 m in length is cut and retrieved in each core barrel; however, on both Legs 106 and 109 shorter or longer intervals were cored depending on engineering requirements. However, on both legs the amount of core recovered was always less than 9 m.

The XCB, first deployed on DSDP Leg 90, was developed in order to recover undisturbed cores in the intermediate zone where the sediment is too hard to be piston cored but too soft to be recovered effectively with the RCB. Rotating with the drill string, the XCB employs a diamond-studded cutting shoe that extends 6 in. below the drill bit and is lubricated by relatively low-energy water jets. This configuration allows the XCB to core soft sediments before they can be washed away by the more energetic drill bit jets. Harder sediments cause the barrel to retract into the drill bit against the pressure of an internal spring, allowing indurated sediments to be cut predominantly by the roller cones and strong water jets of the drill bit.

The cored interval is measured in meters below the seafloor (mbsf). The depth interval assigned to an individual core begins with the depth below the seafloor that the coring operation began and extends to the depth that the coring operation ended. Each coring interval is usually 9.5 m long, the nominal length of

a core barrel; however, the coring interval may be shorter or longer. Cored intervals need not necessarily abut one another but may be separated by drilled intervals. In soft sediment, the drill string may be washed ahead with the core barrel in place but not recovering sediment by pumping water down the drill pipe at high pressure to wash the sediment out of the way of the bit and up the space between the drill pipe and wall of the hole. If thin, hard rock layers are present, it is possible to get "spotty" sampling of these resistant layers within the washed interval, and thus have a cored interval greater than 9.5 m. In drilling hard rock, a center bit may replace the core barrel to drill without core recovery.

Cores taken from a hole are numbered serially from the top of the hole downward (at Hole 648B, the first core recovered on Leg 109 was numbered 7, next in sequence after the last core recovered on Leg 106). Core numbers and their associated cored intervals in meters below seafloor usually are unique in a given hole; however, this may not be true if an interval must be cored twice, due to infall of cuttings or other hole problems. A full-recovery core consists of 9.3 m of rock or sediment contained in a plastic liner (6.6 cm inner diameter) plus about 0.2 m (without a plastic liner) in the core catcher. The core catcher is a device at the bottom of the core barrel, which prevents the core from sliding out when the barrel is being retrieved from the hole.

A recovered core is divided into 1.5-m-long sections that are numbered serially from the top (Fig. 2). When full recovery is obtained, the sections are numbered from 1 through 7, with the last section possibly being shorter than 1.5 m (rarely, an unusually long core may require more than 7 sections). When less than full recovery is obtained, the usual case on Legs 106 and 109, there will be as many sections as needed to accommodate the length of the core recovered; for example, 4 m of core would be divided from the top down into two 1.5-m-long sections and one 1-m-long section. If cores are fragmented (recovery less than 100%), sections are numbered serially with voids preserved,

whether shipboard scientists believe that the fragments were contiguous *in situ* or not. Material recovered from the core catcher is labeled CC and placed below the last section when the core is described. In sedimentary cores, core-catcher recovery is treated as a separate section. Scientists completing visual core description forms (barrel sheets) describe each section as a physical unit; one or more lithologic boundaries may occur anywhere within this physical unit and are not considered when core is sectioned.

A recovered basalt core is cut into 1.5-m-long serially numbered sections also. Each piece of rock is then assigned a number (fragments of a single piece are assigned a single number, with individual fragments being identified alphabetically). The core-catcher sample is placed at the bottom of the last section and is treated as part of the last section, rather than separately. Core and section boundaries are noted only as physical reference points in describing each lithologic unit.

When, as is usually the case, the recovered core is shorter than the cored interval, the top of the core is equated with the top of the cored interval by convention, in order to achieve consistency in handling analytical data derived from the cores. Samples removed from the cores are designated by distance measured in centimeters from the top of the section to the top and bottom of each sample removed from that section. In curated hard-rock sections, sturdy plastic spacers are placed between pieces that do not fit together in order to protect them from damage in transit and in storage; therefore, the centimeter interval noted for a basaltic sample has no direct relationship to that sample's depth within the cored interval but is only a physical reference to the sample's location within the curated core.

A full identification number for a sample consists of the following information: Leg, Site, Hole, Core Number, Core Type, Section Number, Piece Number (for hard rocks), and Interval in centimeters measured from the top of section. For example, a sample identification of "106-648B-5R-3 (Piece 5B, 15-17 cm)" would be interpreted as representing a sample removed from the interval between 15 and 17 cm below the top of Section 3, Core 5 (R designates that this core was taken with the RCB) of Hole 648B during Leg 106, and that this interval fell within Piece 5, Fragment B, of that section.

## Basement Description Conventions

### Visual Core Descriptions

Igneous rock representation on barrel sheets is too compressed to provide adequate information for potential sampling. Consequently, visual core description forms, modified from those used aboard ship, are used for more complete graphic representation. Copies of the visual core description forms, as well as of other prime data collected during Legs 106 and 109, are available on microfilm at all three ODP repositories.

### Core Curation and Shipboard Sampling

Igneous rocks are split into archive and working halves using a rock saw with a diamond blade. A petrologist decides on the orientation of each cut so as to preserve unique features and/or to expose important structures. The archive half is described, and samples for shipboard and shorebased analyses are removed from the working half. On a typical igneous core description form (Fig. 3), the left column is a visual representation of the archive half. A horizontal line across the entire width of this column denotes a plastic spacer glued between rock pieces inside the liner. Each piece is numbered sequentially from the top of each section, beginning with the number 1. Pieces are labeled on the rounded, not the sawn, surface. Pieces that can be fitted together (reassembled like a jigsaw puzzle) are assigned the same number, but are lettered consecutively (e.g., 1A, 1B, 1C, etc.).

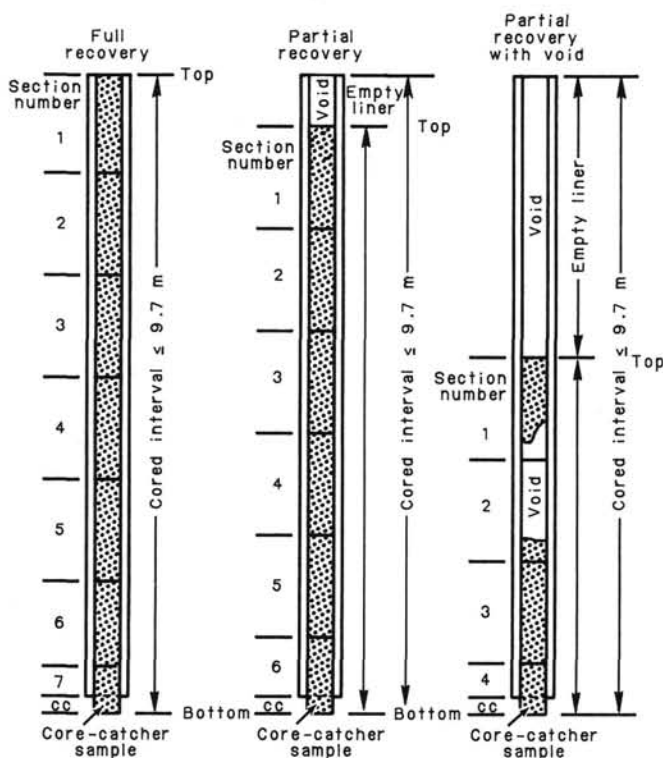
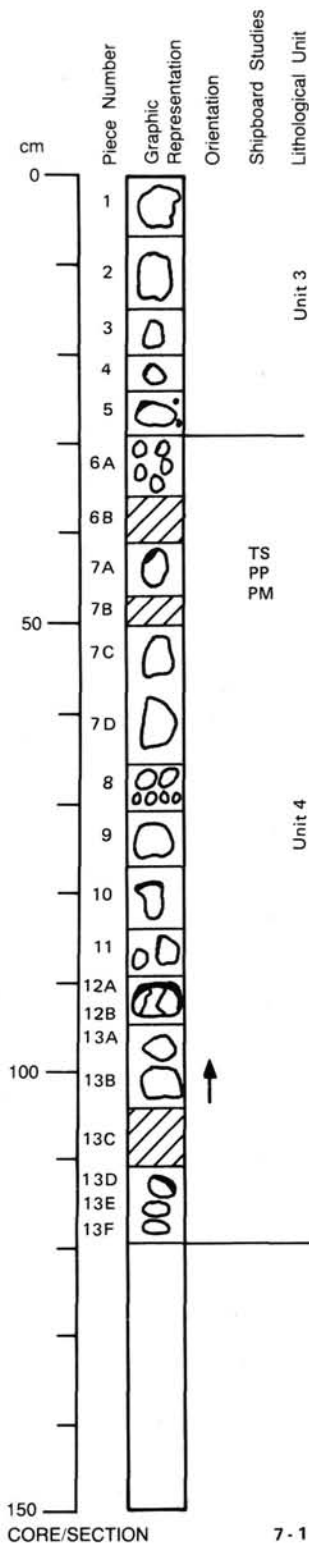


Figure 2. Cutting and labeling of core sections.



**UNIT 3 (continued): HARZBURGITE**

**Pieces 1-5**

**COLOR:** Green.

**LAYERING:** Piece 1 contains layering defined by concentration of orthopyroxene.

Thickness: Indeterminate.

Azimuth and dip: Indeterminate.

Modal layering: Defined by alternating orthopyroxene-rich and olivine-rich layers.

Sequence and abundance: Indeterminate.

Contact: Sharp.

**DEFORMATION:** Foliation defined by long axes of tabular orthopyroxene grains.

Piece 1: Foliation defined by disaggregated and drawn out spinel, and by elongated serpentine halos which extend from orthopyroxene.

**PRIMARY MINERALOGY:**

Olivine - Mode: 85-95%.

Crystal size: <0.2 mm.

Crystal shape: Round.

Preferred orientation: Not apparent.

Percent replacement: Approximately 70% with talc + serpentine + magnetite.

Orthopyroxene - Mode: 3-10%.

Crystal size: As large as 8 mm.

Crystal shape: Round to elliptical.

Preferred orientation: Defined by long axes of elliptical orthopyroxene grains, weak.

Percent replacement: 0-10% with talc, serpentine.

Clinopyroxene - Mode: 1-4%.

Crystal size: As large as 4 mm.

Crystal shape: Round.

Preferred orientation: Not apparent.

Percent replacement: 0%, looks fresh.

Spinel - Mode: 1%.

Crystal size: 1-2 mm.

Crystal shape: Blocky to elliptical.

Preferred orientation: Defined by long axes of some elliptical spinel grains.

Percent replacement: <5% with magnetite.

**SECONDARY MINERALOGY:**

Total percent: 70%.

Texture: Olivine replaced by serpentine, magnetite, and talc in a mesh texture; orthopyroxene pseudomorphed by bastite and rimmed by talc; spinel rimmed by magnetite.

Percent vein material: <1%, <1 mm thick.

Vein material: Most veins are black, possibly magnetite filled; some veins filled by white material, possibly chrysotile.

Figure 3. Igneous visual core description form.

Spacers are placed between pieces with different numbers, but not between those with different letters and the same number. The presence of a spacer may represent a substantial interval of no recovery. Whenever the original unsplit piece is sufficiently large that the top and bottom can be distinguished before re-

moval from the core liner (i.e., the piece could not have rotated about a horizontal axis in the liner during drilling), an arrow is added to the label pointing to the top of the section. Care is taken to ensure that orientation is not lost during the splitting and labeling processes. Oriented pieces are indicated on the de-

scription forms by upward-pointing arrows to the right of the piece. Because pieces are free to turn about a vertical axis during drilling, azimuthal orientation is not possible.

Before the rock is dry sampling is carried out for shipboard physical-properties, magnetics, X-ray diffraction (XRD), X-ray fluorescence (XRF), and thin-section studies. Minicores are taken from the working half and stored in seawater prior to physical-properties measurements. Minicores are subdivided for XRF analysis and thin sectioning, ensuring that as many measurements as possible are made on the same pieces of rock. At least one minicore is taken from each lithologic unit when recovery permits. On the barrel sheets, the type of measurement and approximate sample interval are indicated in the column headed "Shipboard Studies," using the following notation:

XD = X-ray diffraction analysis  
 XF = X-ray fluorescence analysis  
 PM = magnetics measurements  
 TS = thin-section billet  
 PP = physical-properties measurements  
 SEM = scanning electron microscope image  
 P = polished thin section

### Lithologic Description

Lithologic descriptions are prepared in a systematic way, ensuring that all important features (e.g., nature of contacts, distribution and percentage of phenocrysts, groundmass texture, color, vesicles, alteration, etc.) are addressed for each unit described.

### Macroscopic Core Descriptions

Igneous rocks are classified mainly on the basis of mineralogy and texture. When describing the cores, a checklist of macroscopic features is followed to ensure consistent and complete descriptions. Two checklists, one for extrusive rocks and dikes and one for plutonic rocks, are presented below. Figure 3 is an example of a completed igneous visual core description form.

#### Fine-grained and Medium-grained Extrusives and Dikes

Enter leg, site, hole, core number and type, and section information.

Draw the graphic representation of the core, number the rock pieces, and record positions of shipboard samples.

Subdivide the core into lithologic units, using the criteria of changing grain size, occurrence of glassy margins, and changes in petrographic type and phenocryst abundances.

For each lithologic unit, answer the following:

1. Enter UNIT number (consecutive downhole), including piece numbers of top and bottom pieces in unit.
2. ROCK NAME (to be filled in last).
3. CONTACT type (e.g., intrusive, discordant, depositional, etc.). Note the presence of glass and its alteration products (in %), and give the azimuth and dip of the contact.
4. PHENOCRYSTS: determine if distribution is homogeneous or heterogeneous; if distribution is heterogeneous, note variations.

For each phenocryst phase determine:

- a. abundance (%)
- b. average size in mm
- c. shape
- d. degree of alteration (%) and replacing phases and their relationships

- e. further comments
  - f. fill in 2. ROCK NAME (see text following checklist on naming basalts)
5. GROUNDMASS texture: glassy, microcrystalline, fine-grained (< 1 mm), or medium-grained (1–5 mm). Note the relative grain size changes within the unit (e.g., coarsening from Piece 1 to Piece 5).
  6. COLOR (dry).
  7. VESICLES: give percent, size, shape, fillings, relationships (include percent of vesicles filled by alteration minerals), and distribution. Mirols: give percent, size, shape, and distribution.
  8. STRUCTURE: massive, pillow lava, thin flow, breccia, etc., and comments.
  9. ALTERATION: fresh (< 2% alteration); slightly (2%–10%), moderately (10%–40%), highly (40%–80%), very highly (80%–95%), or completely (95%–100%) altered. Type, form, and distribution of alteration.
  10. VEINS/FRACTURES: percent present, width, orientation, fillings and relationships, and halos.

Basalts are termed aphyric, sparsely phyric, moderately phyric, or highly phyric, depending upon the proportion of phenocrysts visible with the hand lens or binocular microscope (approximately  $\times 10$ ). Basalts are called aphyric if phenocrysts clearly amount to less than 1% of the rock, sparsely phyric if phenocryst content ranges from 1% to 2%, moderately phyric at 2%–10%, and highly phyric if phenocrysts amount to more than 10% of the rock. Basalts are further classified by phenocryst type (e.g., a plagioclase-olivine moderately phyric basalt contains 2%–10% phenocrysts, most of them plagioclase but with some olivine).

#### Coarse-grained Plutonics

Enter leg, site, hole, core number and type, and section information.

Draw the graphic representation of the core, number the rock pieces, and record positions of shipboard samples.

Subdivide the core into lithologic units.

For each lithologic unit, answer the following:

1. Enter UNIT number (consecutive downhole), including piece numbers of top and bottom pieces in unit.
2. ROCK NAME (to be filled in last).
3. COLOR (dry).
4. LAYERING:
  - a. if massive, non-layered, or isotropic, skip to 5 on this checklist
  - b. average thickness of different layer types
  - c. azimuth and dip of layering
  - d. types of layering (modal, phase, grain size, graded, rhythmic, cyclic)
  - e. sequence of layers and relative abundance
  - f. layer contacts (sharp, abrupt, smooth, gradational, undulating, rough)
5. DEFORMATION: if rock is deformed, note
  - a. nature and inclination of faults, folds, and shear and/or brecciated zones
  - b. nature and inclination of foliations and lineations
  - c. features that define the foliation or lineation
  - d. grain size variations due to granulation and/or recrystallization
6. PRIMARY MINERALOGY, including intergranular and granular phases. Note for each phase, in order of modal abundance
  - a. modal percent
  - b. range of crystal sizes

- c. crystal shapes
  - d. preferred orientations
  - e. percent replacement with what replacement mineral
7. SECONDARY MINERALOGY
- a. total percent secondary phases
  - b. textures of secondary phases
  - c. vein material: note total percent vein material, average vein thickness, and types and textures of filling
8. Note ADDITIONAL FEATURES.

Whenever possible, peridotites are classified according to their primary mineralogy. If no primary minerals can be identified because of extensive serpentinization, the serpentinized peridotites are called serpentinites. In the case of partially serpentinized samples, the term "serpentinized" is used to modify the rock name (e.g., serpentinized harzburgite). In some serpentinites, serpentine minerals closely pseudomorph primary minerals (e.g., lizardite replacing orthopyroxene in bastite). The primary mineralogy of these samples is estimated from the abundances of various pseudomorph types.

#### *Thin-Section Descriptions*

Thin-section billets of basaltic rocks recovered during Legs 106 and 109 were examined to help define unit boundaries indicated by hand-specimen core descriptions, to confirm the identity of the petrographic groups represented in the cores, and to define their secondary alteration mineralogy. A least one thin section was made of each unit identified in hand specimen where sufficient rock was available.

In accordance with the procedures generally adopted by petrologists during earlier DSDP legs, the petrographic units identified in thin section are described strictly by the presence of phenocryst assemblages or an individual phenocryst phase but not by the relative abundance of phases as in the hand-specimen descriptions. Percentages of individual phenocryst phases are estimated visually and reported on the detailed thin-section description sheets. Modal abundances determined by point counting are reported in the "Petrography" sections of each site chapter. The terms sparsely, moderately, and highly phyrlic are used in the same manner as for hand-specimen descriptions. In cases where discrepancies arise over the composition and abundance of phenocryst phases between hand-specimen and thin-section analyses, thin-section descriptions are used in preference to hand-specimen descriptions in the "Lithostratigraphy" sections.

#### *Basement Alteration*

Alteration effects due to seawater interaction with igneous rocks were described in hand specimens and thin section. The width and color of any alteration halos around fractures or vugs were noted in the core descriptions. The identities of secondary minerals filling fractures, vesicles, and replacing igneous phases were estimated in core descriptions and refined in thin section, augmented in some cases by XRD and electron-probe analyses made on shipboard thin sections. The total percentages of the various secondary minerals were also estimated from thin-section examinations.

#### **Preservation of Samples from the Hydrothermal Vent Area**

Sulfide minerals, particularly fine-grained, disseminated material, are susceptible to oxidation. In order to reduce the rate at which the material collected at Site 649 was altered, the following preservation procedure was followed.

1. Archive halves: Archive halves were placed in heat-shrink plastic tubing and purged with nitrogen. The heat-shrink tubing

was shrunken onto the core tubes with a heat gun. The process was repeated with a second heat-shrink tube.

2. Working halves: Working halves were sampled every 30 cm, where appropriate, into 20-cm<sup>3</sup> scoop samples. These samples were dried in the freeze dryer, purged with nitrogen, and heat sealed in plastic bags. The scoop samples were returned to the working halves for storage. The working halves were purged with nitrogen, sealed in one layer of heat-shrink tubing, and stored in D-tubes.

3. Core 106-649E: The only sample taken from Core 106-649E was a 20-cm<sup>3</sup> scoop sample. This sample was divided into three roughly equal parts. One part was sealed in a low-permeability KAPAK bag filled with seawater to protect dehydrated phases. Another part was dried in the freeze dryer, placed in a KAPAK bag, purged with nitrogen, and sealed. The third part was placed in a Kimble Colorbreak vial, dried in the freeze dryer, evacuated with a rotary pump, and sealed by fusing the top of the glass vial. The result of this process is that Core 106-649E has material stored in four different ways.

The probability that these cores will suffer extensive alteration upon storage is high. Both atmospheric oxygen and the water in the wet core material will cause oxidation. Core curators should consider a systematic repackaging of this material, particularly in the case of the archive halves, which will remain untouched for many years. Rebagging, dry, in KAPAK bags filled with nitrogen is probably a suitable technique.

Because working halves will be reopened frequently, some consideration should be given to restricting sampling to, perhaps, twice a year in order to minimize exposure to the atmosphere and prevent rapid degradation of the core material, which should remain sealed when not being sampled.

#### **XRD ANALYSES**

A Philips ADP 3520 X-ray diffractometer was used for the XRD analysis of unknown secondary mineral phases. Instrument conditions were as follows:

CuK $\alpha$  radiation with Ni filter  
 40 kV  
 35 mA  
 Goniometer scan from 2° to 50° 2 $\theta$   
 Step size 0.02°  
 Count time 2 s

Samples were prepared by grinding under water in an agate pestle and mortar until reduced to a very fine slurry. A suspension was then pipetted onto the surface of a glass slide and allowed to air dry before X-ray analysis. In some cases, a centrifuge was used to reduce the amount of primary minerals in the suspension. Ethylene glycol solution was used to identify clay minerals.

Resulting diffractograms were interpreted with the help of a computerized search and match routine using JCPDS powder files and tabulated data for clay minerals in Brindley and Brown (1980).

#### **XRF ANALYSES**

Samples considered by the shipboard party to be representative of individual lithologic units, or possibly of unusual composition, were analyzed for major and trace elements by X-ray fluorescence (XRF). The on-board XRF system (A.R.L. 8420) is a fully automated, wavelength-dispersive, X-ray fluorescence spectrometer using a 3-kW rhodium X-ray tube as the excitation source for both major and trace elements. The current list of analyzed elements and operating conditions is given in Table 1.



**Table 1. Operation conditions for the XRF.**

Element	Peak	2 $\beta$	Goniometer	Crystal	Detector <sup>a</sup>	Collimator <sup>b</sup>	Threshold and window settings <sup>c</sup>	Total count time (s)
Si	K $\alpha$	109.226	2	PET	FPC	C	43	40
Ti	K $\alpha$	86.144	2	LiF200	FPC	F	53	40
Al	K $\alpha$	145.133	2	PET	FPC	C	44	40
Fe	K $\alpha$	57.526	2	LiF200	FPC	F	52	40
Mn	K $\alpha$	62.967	1	LiF200	Kr	F	44	40
Mg	K $\alpha$	44.880	2	TLAP	FPC	C	33	200
Mg Bg		45.680	2	TLAP	FPC	C	33	100
Ca	K $\alpha$	113.149	2	LiF200	FPC	C	44	40
Na	K $\alpha$	54.723	2	TLAP	FPC	C	35	200
Na Bg		53.723	2	TLAP	FPC	C	35	100
K	K $\alpha$	136.665	2	LiF200	FPC	F	44	40
P	K $\alpha$	141.040	2	Ge	FPC	C	43	100
Rb	K $\alpha$	26.600	1	LiF200	SC	F	35	60
Rb Bg		26.600	1	LiF200	SC	F	35	30
Sr	K $\alpha$	25.139	2	LiF200	SC	F	22	60
Sr Bg		24.639	2	LiF200	SC	F	22	30
Sr Bg		25.639	2	LiF200	SC	F	22	30
Zr	K $\alpha$	22.532	2	LiF200	SC	F	22	60
Zr Bg		21.712	2	LiF200	SC	F	22	30
Zr Bg		22.972	2	LiF200	SC	F	22	30
Y	K $\alpha$	23.776	1	LiF200	SC	F	35	60
Y Bg		23.076	1	LiF200	SC	F	35	30
Y Bg		24.176	1	LiF200	SC	F	35	30
Nb	K $\alpha$	21.375	1	LiF200	SC	F	33	200
Nb Bg		21.037	1	LiF200	SC	F	33	75
Nb Bg		21.713	1	LiF200	SC	F	33	75
Ni	K $\alpha$	48.669	2	LiF200	SC	C	35	60
Ni Bg		47.869	2	LiF200	SC	C	35	30
Ni Bg		49.469	2	LiF200	SC	C	35	30
V	K $\alpha$	76.953	2	LiF200	FPC	F	52	60
V Bg		75.953	2	LiF200	FPC	F	52	30

Note: All elements were analyzed at 60 kV and 50 mA. Bg = background.

<sup>a</sup> FPC: Flow proportional counter; SC: scintillation counter; Kr: Kr detector.

<sup>b</sup> C = coarse collimator; F: fine collimator.

<sup>c</sup> See A.R.L. software manuals.

Because the XRF lab aboard *JOIDES Resolution* is a relatively new addition, much of the laboratory work on Legs 106 and 109 was aimed at developing sample preparation techniques and data reduction routines that are flexible and streamlined enough to provide high-quality chemical data to the shipboard scientists.

### Crushing and Grinding

Sample preparation begins by taking approximately 10 cm<sup>3</sup> of rock and removing any saw marks or unwanted material by wet-grinding on a silicon carbide disk mill. Each sample is then ultrasonically washed in distilled water and methanol for 10 min and dried at 110°C for at least 2 hr. Larger pieces are reduced to less than 1 cm diameter by crushing between two plastic disks in a hydraulic press. Powders were produced by grinding pieces less than 1 cm in diameter in a motorized agate mortar and pestle for 10 to 30 min to minimize contamination (Thompson and Bankston, 1970).

### Major Elements

Major elements are determined on fused glass disks in order to reduce matrix effects and variations in background (Claisse, 1956; Rose et al., 1962; Norrish and Hutton, 1969). These disks are made by mixing 6.00 g of dry, lanthanum-doped (20% La<sub>2</sub>O<sub>3</sub>), lithium tetraborate flux (Spex #FF28-10) with 0.500 g of rock powder that has been ignited at 1000°C in platinum-gold crucibles for 6–10 min and then poured into Pt-Au molds using a modified Claisse Fluxer apparatus. This 12:1 flux-to-sample ratio reduces matrix effects to the point where matrix corrections are unnecessary for normal basaltic to granitic compositions. Therefore, simple linear relationships exist between X-ray inten-

sities and oxide concentrations for most elements, and major element concentrations are easily calculated using the equation:

$$C_i = (I_i \times m_i) - b_i$$

Where

$C_i$  = concentration (wt%) of oxide  $i$

$I_i$  = net peak intensity (cps) of oxide  $i$

$m_i$  = slope of calibration curve (wt%/cps) of oxide  $i$

$b_i$  = measured blank (wt%) of oxide  $i$

Slope ( $m_i$ ) is determined by measuring both natural and synthetic standards, and calculating a simple linear regression, with the aid of graphs to help identify anomalous numbers. A measured blank ( $b_i$ ) is used in place of a blank derived from a regression. For most major elements, this makes little difference. For minor elements such as K<sub>2</sub>O and P<sub>2</sub>O<sub>5</sub>, where concentrations often approach background levels, better results are achieved by measuring blanks on synthetic and natural standards. Because of low count rates, backgrounds were measured on all unknowns for MgO and Na<sub>2</sub>O, rather than only on a blank. When extreme compositions are to be determined, such as MgO in ultramafic rocks, standards closer in composition to the unknowns should be used.

### Trace Elements

Trace elements are determined on pressed-powder pellets made by mixing 6 g of fresh rock powder with 1 g of wax. This mixture is then pressed into an aluminum cap with 7 tons of pressure. A minimum of 5 g of sample ensures the pellet will be "infinitely thick" for rhodium K-series radiation.

To compute trace element concentrations from measured X-ray intensities, an off-line calculation program based on routines from Bougault et al. (1977) was written by T. L. Grove and M. Loubet. Dead-time corrected X-ray intensities for peaks and backgrounds from an A.R.L. result file are corrected for machine drift by using a one-point correction of the form:

$$D_i = S_i/M_i$$

$$I_{di} = I_i \times D_{ip}$$

Where

$D_i$  = drift factor for element  $i$ , generally  $1.00 \pm 0.01$

$S_i$  = peak intensity for element  $i$ , measured on synthetic standard MERD at time of calibration

$M_i$  = measured peak intensity for element  $i$ , measured on MERD at any time after the calibration

$I_i$  = uncorrected peak or background intensity, element  $i$

$I_{di}$  = drift-corrected peak or background intensity, element  $i$

Peak intensities were linearly corrected for background.

To correct for matrix differences between samples, three separate mass absorption coefficients are determined following a modification of the Compton scattering technique of Reynolds (1967). Measured intensities from the rhodium K-series Compton,  $Fe_{K\alpha}$ , and  $Ti_{K\alpha}$  lines are compared to the calculated absorption coefficients of Rb ( $A_{Rb}$ ), Cr ( $A_{Cr}$ ), and V ( $A_V$ ), respectively. From this comparison, three equations of the form:

$$A_{Rd} = 10^4 / ([Rh_{cps} \times A] + B)$$

$$A_{Cr} = A_{Rb} / ([Fe_{cps} \times C] + D)$$

$$A_V = A_{Cr} / ([Ti_{cps} \times E] + F)$$

can be written to describe the relationship between each coefficient and its respective line. Using this method, unknowns can be measured and corrected for matrix differences without calculating the absorption coefficients for each sample.

Trace element concentrations were calculated using the empirical formula (Bougault et al., 1977):

$$(I - I_0)M = AC + C'C' + B$$

Where

$I$  = background and drift corrected peak intensity

$I_0, B$  = constants that take instrument interferences and non-linearity of background into account

$A$  = mass absorption coefficients for the element of interest

$A'$  = mass absorption coefficient for an interfering element

$C$  = concentration of the element of interest

$C'$  = concentration of an interfering element

Constants for this equation were determined using N natural rock standards and solving N linear equations of the above form.

## PHYSICAL PROPERTIES

The following physical-properties measurements were made routinely on board the ship, for Hole 648B basalt cores, although not all of the properties were measured for each core:

Bulk density (GRAPE 2-min count)

Thermal conductivity (half-space needle probe)

Compressional wave velocity (Hamilton Frame)

Index properties (bulk density, porosity, water content, and grain density)

Standard procedures were invoked for the measurements as described below and in the appended references.

### GRAPE Bulk Density

The Gamma Ray Attenuation Porosity Evaluator (GRAPE) was used to determine the density of discrete samples of basalt. In all cases the sample was positioned between a shielded gamma-ray source and a shielded scintillation detector. The beam attenuation is primarily due to Compton scattering and, as such, is directly related to the material's density. The principles of technique are thoroughly described by Evans (1965), while its application to (DSDP) ODP, together with the necessary calibration procedures, are documented by Boyce (1976).

### 2-Minute Counts

In this static mode a discrete sample of material is placed between the source and detector, and the number of counts is monitored over a 2-min period. Consideration of this value in relation to the sample thickness and associated calibration results enable determination of a value for the bulk density. The whole system is calibrated empirically using a quartz standard, and the computed bulk density of the sample is corrected for deviations from this standard value by inputting the true grain density determined by conventional gravimetric and volumetric techniques (calibration done on Leg 106 only).

### Compressional-Wave Velocity (Hamilton Frame)

Compressional-wave velocity measurements were also made using the Hamilton Frame. These measurements were made on the minicores of basalt and samples of sediment taken for paleomagnetic analyses and index properties determinations. The design and operating procedure is described by Boyce (1976). Calibration of the device was undertaken using aluminum and Plexiglas standards.

### Index Properties

This suite of data comprises gravimetric and volumetric determinations used to evaluate the parameters of wet and dry densities, porosity, water content, void ratio, and grain density. Minicores of rock were used exclusively. Wet and dry weights were determined on board using the motion-compensated Scitech electronic balance to an accuracy of  $\pm 0.01$  g. Sample volumes were determined for both the wet and dry specimens using the penta-pycnometer (Leg 106 only). This apparatus is designed for the precise evaluation of volumes of dry powders and as such works well for dry samples.

### Thermal Conductivity

Thermal-conductivity measurements were made on the basalt samples from Holes 648B and 669A and on samples of serpentinites and serpentized harzburgites from Hole 670A. The basalt samples were taken mainly from the same piece as the minicore used for the other physical-properties measurements. The measurements were done with the modified half-space needle-probe device (Thermcon 85). The measurement method is based on an application of the infinite line source principle, as given by Von Herzen and Maxwell (1959).

### Hard-Rock Paleomagnetism

Paleomagnetic measurements were performed on minicore samples taken from selected areas within the recovered cores. These areas were chosen on the basis of lithologic homogeneity and the ability to orient the samples with respect to the vertical direction. When possible, at least one shipboard sample was

taken from each core section (1.5 m). However, some sections were not sampled at all, as much of the recovered core consisted of unoriented fragments and drilling rubble.

Magnetic susceptibility ( $X_0$ ) was measured using a Bartington Magnetic Susceptibility Meter (Model MS1). This value of initial susceptibility was used in conjunction with natural remanent magnetism (NRM) values to calculate the Q ratio (Könisberger) of the samples. In this calculation a field value of 0.4 Oe was assumed so that

$$Q = \frac{\text{NRM}}{(X_0 \times 0.4)}$$

Remanent magnetization was measured with a MOLSPIN Portable Rock Magnetometer. For Leg 109, the spinner-type magnetometer was interfaced to a DEC PRO-350 microcomputer using software written by Y. Hamano. Stepwise alternating-field (AF) demagnetization was performed with a single-axis Schonstedt Geophysical Specimen Demagnetizer (Model GSD-1) in steps until the specimen fell below the median destructive field (MDF) and a stable inclination was identified on the Zijderveld plot.

#### REFERENCES

- Bougault, H., Cambon, P., and Toulhoat, H., 1977. X-ray spectrometric analysis of trace elements in rocks; Correction for instrumental interferences. *X-Ray Spectrom.*, 6(2):66-72.
- Boyce, R. E., 1976. Definitions and laboratory techniques of compressional sound velocity parameters and wet-water content, wet-bulk density, and porosity parameters by gravimetric and gamma-ray attenuation techniques. In Schlager, S. O., Jackson, E. D., et al., *Init. Repts. DSDP*, 33: Washington (U.S. Govt. Printing Office), 931-958.
- Brindley, G. W., and Brown, G. (Eds.), 1980. Crystal structures of clay minerals and their X-ray identification. *Mineral. Soc. Monogr.*, 5.
- Claissé, F., 1956. Accurate X-ray fluorescence analysis without internal standard. *Quebec Dept. Mines Press Release* 327.
- COSOD, 1981. Conference on scientific ocean drilling: Washington (Joint Oceanographic Institutions, Inc.).
- Detrick, R. S., and Purdy, G. M., 1980. The crustal structure of the Kane Fracture Zone from seismic refraction studies. *J. Geophys. Res.*, 85:3759-3778.
- Evans, H. B., 1965. GRAPE-A device for continuous determination of material density and porosity. *Trans. SPWLA Annu. Logging Symp.*, 6th, Dallas, 2:B1-B25.
- Honnorez, J., Von Herzen, R. P., et al., 1983. *Init. Repts. DSDP*, 70: Washington (U.S. Govt. Printing Office).
- Macdonald, K. C., 1982. Mid-Ocean ridges: Fine scale tectonic, volcanic and hydrothermal processes within the plate boundary zone. *Annu. Rev. Earth Planet. Sci.*, 10:115-190.
- Natland, J. H., and Rosendahl, B. R., 1980. Drilling difficulties in basement drilling during Deep Sea Drilling Project Leg 54. In Rosendahl, B. R., Hekinian, R., et al., *Init. Repts. DSDP*, 54: Washington (U.S. Govt. Printing Office), 593-603.
- Norrish, K., and Hutton, J. T., 1969. An accurate X-ray spectrophotographic method for the analysis of a wide range of geological samples. *Geochim. Cosmo. Acta*, 33:431-453.
- Reynolds, R. C., 1967. Estimation of mass absorption coefficients by Compton scattering: Improvements and extrusions of the method. *Am. Mineral.*, 48:1133-1143.
- Thompson, G., and Bankston, D. C., 1970. Sample contamination from grinding and sieving determined by emission spectroscopy. *Appl. Spectros.*, 24:210-219.
- Von Herzen, R. P., and Maxwell, A. E., 1959. The measurement of thermal conductivity of deep-sea sediments by a needle probe method. *J. Geophys. Res.*, 64:1557.